

## Microencapsulation of phosphate: application to flame retarded coated cotton

Stephane Giraud<sup>a</sup>, Serge Bourbigot<sup>a,\*</sup>, Maryline Rochery<sup>a</sup>, Isabelle Vroman<sup>a</sup>,  
Lan Tighzert<sup>b</sup>, Rene Delobel<sup>c</sup>

<sup>a</sup>Laboratoire de Génie et Matériaux Textiles (GEMTEX), UPRES EA2161, Ecole Nationale Supérieure des Arts et Industries Textiles (ENSAIT),  
9 rue de l'Ermitage, BP 30329, 59056 Roubaix cedex 01, France

<sup>b</sup>Laboratoire de Chimie Macromoléculaire (LCM), UPRESA-CNRS 8009, Université des Sciences et Technologies de Lille (USTL)—Bât. C6,  
59655 Villeneuve d'Ascq cedex, France

<sup>c</sup>Centre de Recherche et d'Étude sur les Procédés d'Ignifugation des Matériaux (CREPIM), Parc de la Porte Nord—Rue Christophe Colomb,  
62700 Bruay La Buisnière, France

Received 19 October 2001; received in revised form 18 January 2002; accepted 3 February 2002

### Abstract

Polyurethane-phosphates combination is known to form a flame retardant (FR) intumescent system. The intumescent formulation could not be permanent because of the water solubility of the phosphate. This problem could be solved by the technique of microencapsulation. Di-ammonium hydrogen phosphate (DAHP) was microencapsulated with a polyurethane (PU) shell. Polyurethane for textile coating was loaded with neat or microencapsulated DAHP. We studied the thermal degradation behaviour of DAHP microcapsules, PU loaded formulations and cotton coated by these PU formulations. Improvement of the thermal stability for PU textile coating was observed with neat and microencapsulated DAHP. The flame retarding behaviour of these coated cotton fabrics was also valued with the cone calorimeter. This new concept of phosphate encapsulated by PU shell showed a significant FR effect. © 2002 Elsevier Science Ltd. All rights reserved.

**Keywords:** Polyurethane; Microencapsulation; Phosphate; Intumescence; Thermal degradation; Textile; Coating; Cotton

### 1. Introduction

Textile coating with polyurethane (PU) resins provides to fabric properties such as abrasion resistance, water repellent, leather aspect etc. This type of coating on cotton or cotton-polyester blended fabrics is used in many fields such as transportation industry (e.g. car seats), garments (e.g. waterproof breathable jackets), furniture (e.g. artificial leather), but these PU coatings have a bad flame retardancy.

The addition of a flame retardant in PU coating is necessary to improve the fire behaviour of materials. According to several reports [1–4], ammonium phosphates are efficient to develop with PU a flame retardant (FR) intumescent system. Intumescent formulations with ammonium phosphates are unfortunately not permanent.

Indeed, ammonium phosphates are water-soluble and they have a poor compatibility with the polymer. Thus problems of migration and solubility may occur. The microencapsulation of ammonium phosphates could avoid these problems. Microencapsulation is a process of enveloping microscopic amounts of matter in a thin film of polymer, which forms a solid wall [5]. This core/shell structure allows isolation of the encapsulated substance from the surroundings and thus protects it from any degrading factors such as water. The encapsulated substance can be liberated by fusion or dissolution of the impermeable shell or by diffusion across a porous shell [6,7].

It is of interest to study microencapsulation with a polyurethane shell for two main reasons. First, we can expect that microcapsules with PU shell will be compatible with the final PU coating on textiles and also with other polymeric matrices. Second, combination of the encapsulated ammonium phosphates and the PU shell could be itself an efficient FR intumescent formulation,

\* Corresponding author. Tel.: +33-3-20-25-89-84; fax: +33-3-20-27-25-97.

E-mail address: serge.bourbigot@ensait.fr (S. Bourbigot).

which could be introduced in different types of textiles or materials in order to protect them. In previous work [8], we synthesised microcapsules containing di-ammonium hydrogen phosphate (DAHP) with a polyurethane shell by the technique of interfacial polycondensation [9–11]. The microcapsules obtained are almost spherical with a number-average diameter of about 1  $\mu\text{m}$  and a number-average particle size distribution lower than 5  $\mu\text{m}$ . This new concept of encapsulated phosphate used as intumescent additive was shown. We demonstrated using cone calorimeter that reaction to fire of cotton fabrics coated by PU containing encapsulated phosphate was efficient.

In this work, several formulations of PU with different loading of encapsulated DAHP or neat DAHP and also cotton fabrics coated by these different FR PU formulations are examined by thermal analysis. The reaction to fire of these different coated cotton fabrics is also studied using the cone calorimeter as a fire model [12,13].

## 2. Experimental

### 2.1. Materials

Raw materials were used without further purification. A pure cotton fabric (146  $\text{g m}^{-2}$ ) was coated by a commercial PU paste from Allrim obtained from a mixture of 100 parts of polyol (polyol AW) and 140 parts of MDI prepolymer (isocyanate BY). We introduced in this paste 15 to 50% (by weight) of neat DAHP,  $(\text{NH}_4)_2\text{HPO}_4$  (purity 99% minimum) from Riedel-de Haën AG, or 15–40% of DAHP microcapsules synthesised in our laboratory [8]. The polyurethane shell of these microcapsules is synthesised from diphenyl methylene diisocyanate (blend of MDI isomers, 4,4'-diphenyl methylene diisocyanate principally) and polyethylene glycol with a number average molecular weight of 400  $\text{g mol}^{-1}$  (PEG 400). We synthesised also microcapsules with the same PU shell but without DAHP in order to study the thermal behaviour of this PU shell.

### 2.2. Coating processing

Coatings were carried out by using a coating table K Control Coater (Erichsen). This coating technique is close to coating with a scraper, except the coated support is fixed and the coating paste is spread with a threaded rod. The coating thickness increases with the threading size of the rod. We used a rod with a medium thread to obtain an expected coating thickness of 36  $\mu\text{m}$ . The weight of deposited coating was about 210  $\text{g m}^{-2}$ . The coated fabric was placed in a drying oven at 80  $^\circ\text{C}$  for 4 h.

The various formulations of PU coating are described in Table 1. We compared the PU coatings including

encapsulated DAHP with those including neat DAHP, at different loading ratios.

### 2.3. TGA experiment

All TGA tests were carried out using TGA 2950 from TA Instruments at a linear heating rate of 10  $^\circ\text{C min}^{-1}$  under air 60  $\text{ml min}^{-1}$  (Alphagaz from Air Liquide). The weight of all samples was kept within 9–10 mg. The temperature range was from ambient to 800  $^\circ\text{C}$  (all the graphs are presented from 100  $^\circ\text{C}$ ). Concerning thermal analysis of PU formulations and PU coatings, curves of weight difference between the experimental and theoretical TG curves are computed as follows:

$W_{\text{exp}}(T)_{\text{PU}}$ : TG curve of neat commercial PU for textile coating,

$W_{\text{exp}}(T)_{\text{loading}}$ : TG curve of neat loading (neat or encapsulated DAHP),

$W_{\text{exp}}(T)_{[\text{PU/loading}]}$ : TG curve of the blend PU/neat or encapsulated DAHP,

$W_{\text{th}}(T)_{[\text{PU/loading}]}$ : theoretical TG curve computed by linear combination between the TG curves of PU and loading where  $x$ ,  $y$  are the weight percentage of PU and loading in the blend.

$W_{\text{th}}(T)_{[\text{PU/loading}]} = x \cdot W_{\text{exp}}(T)_{\text{PU}} + y \cdot W_{\text{exp}}(T)_{\text{loading}}$ ;  
 $x + y = 1$

$\Delta(T)_{[\text{PU/loading}]}$ : curve of weight difference:

$\Delta(T)_{[\text{PU/loading}]} = W_{\text{exp}}(T)_{[\text{PU/loading}]} - W_{\text{th}}(T)_{[\text{PU/loading}]}$

$W_{\text{exp}}(T)_{\text{cotton}}$ : TG curve of neat cotton fabric,

$W_{\text{exp}}(T)_{[\text{cotton/PU/loading}]}$ : TG curve of cotton coated by the blend PU/neat or encapsulated DAHP,

$W_{\text{th}}(T)_{[\text{cotton/PU/loading}]}$ : theoretical TG curve computed by linear combination between the TG curves of cotton, PU and loading where  $x$ ,  $y$ ,  $z$  are the weight percentage of PU, loading and cotton.

$W_{\text{th}}(T)_{[\text{cotton/PU/loading}]} = x \cdot W_{\text{exp}}(T)_{\text{PU}}$   
 $+ y \cdot W_{\text{exp}}(T)_{\text{loading}} + z \cdot W_{\text{exp}}(T)_{\text{cotton}}$ ;  
 $x + y + z = 1$

$\Delta(T)_{[\text{cotton/PU/loading}]}$ : curve of weight difference:

Table 1  
Different coating formulations tested

Formulation name	Composition of coating on cotton fabrics
cotton + virgin PU	PU (reference sample)
cotton + 80/20 PU-DAHP	PU with 20 wt.% neat DAHP
cotton + 60/40 PU-DAHP	PU with 40 wt.% neat DAHP
cotton + 50/50 PU-DAHP	PU with 50 wt.% neat DAHP
cotton + 85/15 PU- $\mu$ DAHP	PU with 15 wt.% microcapsules of DAHP
cotton + 70/30 PU- $\mu$ DAHP	PU with 30 wt.% microcapsules of DAHP
cotton + 60/40 PU- $\mu$ DAHP	PU with 40 wt.% microcapsules of DAHP

$$\Delta(T)_{[\text{cotton/PU/loading}]} = W_{\text{exp}}(T)_{[\text{cotton/PU/loading}]} - W_{\text{th}}(T)_{[\text{cotton/PU/loading}]}$$

The  $\Delta T$  curves allow the observation of an eventual increase or decrease in the thermal stability of the formulations compared to the combination of components analysed separately.

#### 2.4. Cone calorimeter

Our samples were exposed in a Stanton Redcroft Cone calorimeter following the procedure defined in ASTM E 1354. They were put in horizontal orientation between two cut steel sheets. The surface exposed to the external heat flux was  $9 \times 9 \text{ cm}^2$ . The external heat flux chosen was  $35 \text{ kW m}^{-2}$  because it corresponds to a common heat flux in a mild fire scenario. We obtained conventional data on principal fire properties using software developed in our laboratory: rate of heat released (RHR), cumulative heat released (total heat evolved: THE), volume of smoke production (VSP) [14], CO and CO<sub>2</sub> production, and FIGRA (Fire Growth Rate) index [15]. VSP measures the flow of smoke in a ventilated room. FIGRA, computed as  $\text{FIGRA} = \text{RHR} (W)/\text{Time} (s)$ , provides an estimate of both the spread (rate) and the size of a fire. The experiments were repeated 3 times. When measured at  $35 \text{ kW m}^{-2}$  flux, RHR and VSP values are reproducible to within  $\pm 10\%$  and weight loss, CO, CO<sub>2</sub> are reproducible to within  $\pm 15\%$ . The results presented here are the average of three measurements. The cone data reported in this work are the average of three replicated experiments.

### 3. Results and discussion

#### 3.1. Thermal degradation study

The thermal behaviour of DAHP microcapsules was studied. TG curves of the neat DAHP, encapsulated DAHP and the virgin PU shell (microcapsule without DAHP) are reported in Fig. 1. The weight loss of neat DAHP starts at  $100 \text{ }^\circ\text{C}$  and corresponds to evolving adsorbed water. The peak at  $200 \text{ }^\circ\text{C}$  of the weight loss rate can be assigned to ammonia. At higher temperature, DAHP is transformed into polyphosphoric acid (PPA) [16] and then, PPA dehydrates to phosphorus oxides ( $\text{P}_4\text{O}_{10}$  type). At  $500 \text{ }^\circ\text{C}$ ,  $\text{P}_4\text{O}_{10}$  is sublimed. No residue is observed at  $550 \text{ }^\circ\text{C}$ . Neat PU shell of microcapsules without DAHP degrades in two main steps. The first starts at  $200 \text{ }^\circ\text{C}$  with a peak of weight loss rate ( $9\% \text{ min}^{-1}$ ) at  $280 \text{ }^\circ\text{C}$  and the second starts at  $400 \text{ }^\circ\text{C}$  with a peak of weight loss ( $6\% \text{ min}^{-1}$ ) at  $530 \text{ }^\circ\text{C}$ . No residue is observed at  $600 \text{ }^\circ\text{C}$ . The TGA curve is similar to the one obtained by Grassie and Perdomo Mendoza [17] for a polyurethane derived from MDI and PEG of

molar mass 200. These authors identified the onset of degradation with the depolymerisation of the urethane bonds to produce the starting monomers. Under atmospheric pressure, the monomers volatilise only slowly from the condensed phase and undergo a series of further reactions, some of which are scission reactions that produce more volatile chain fragments and rearrangement products (for example, acetaldehyde from the PEG sequences and carbodiimide formed by dimerization of newly formed isocyanates with evolving CO<sub>2</sub>). The decomposition of encapsulated DAHP is rather more complex and shows more than two stages. The weight loss starts at  $140 \text{ }^\circ\text{C}$  with water evolution. Then the second step of weight loss corresponds to ammonia evolving from DAHP and at the same time the degradation of PU. PU shell of DAHP microcapsules degrades earlier than neat PU shell. Indeed the depolycondensation is catalysed by acidity from decomposition of DAHP. Several studies [18–21] showed the intumescent mechanism between phosphorus compounds and polyurethane. Polyphosphoric acid accelerates and increases the formation of char by carbonisation and additional crosslinking reactions, also the quantity of inflammable volatile products is decreased. Thus, for PU shell of DAHP microcapsules, the first peak of weight loss rate is delayed at  $320 \text{ }^\circ\text{C}$  instead of  $280 \text{ }^\circ\text{C}$  for neat PU shell and this peak of weight loss rate is smaller ( $4\% \text{ min}^{-1}$ ) than one of neat PU shell ( $9\% \text{ min}^{-1}$ ). The thermal stability is slightly enhanced (temperature range  $300\text{--}800 \text{ }^\circ\text{C}$ ) and a residue of 5 wt.% is observed at  $650 \text{ }^\circ\text{C}$ .

Fig. 2 shows the TG curves of the commercial PU for textile coating alone and with different DAHP or encapsulated DAHP loading: 40 or 50 wt.% of neat DAHP and 30 or 40 wt.% of encapsulated DAHP. For the degradation of commercial PU, one finds again the two main steps described previously for PU of microcapsule shell. But the commercial PU degrades faster than the neat PU shell, the first step has a really important peak of weight loss rate ( $22\% \text{ min}^{-1}$ ) at  $325 \text{ }^\circ\text{C}$ . The char residue is 15% at  $450 \text{ }^\circ\text{C}$  and 0% at  $600 \text{ }^\circ\text{C}$ . The degradation for the four formulations of commercial PU loaded is similar, with three main steps. The first takes place at  $200 \text{ }^\circ\text{C}$  and corresponds to evolving ammonia and the start of PU decomposition by DAHP. This weight loss is inversely proportional to the loading of DAHP (at  $200 \text{ }^\circ\text{C}$ , 6.5% for the biggest load, 50/50 PU-DAHP formulation, and 1.5% for the weakest load, 70/30 PU- $\mu$ DAHP formulation). The two next steps can be assigned to the two degradation steps of commercial PU. In the temperature range  $200\text{--}300 \text{ }^\circ\text{C}$ , the loaded PU formulations decompose faster than neat commercial PU, because the decomposition of DAHP catalyses the depolycondensation of PU. Then the products from DAHP decomposition react with starting monomers of PU to decrease production of inflammable volatile compounds and to increase at higher temperature the

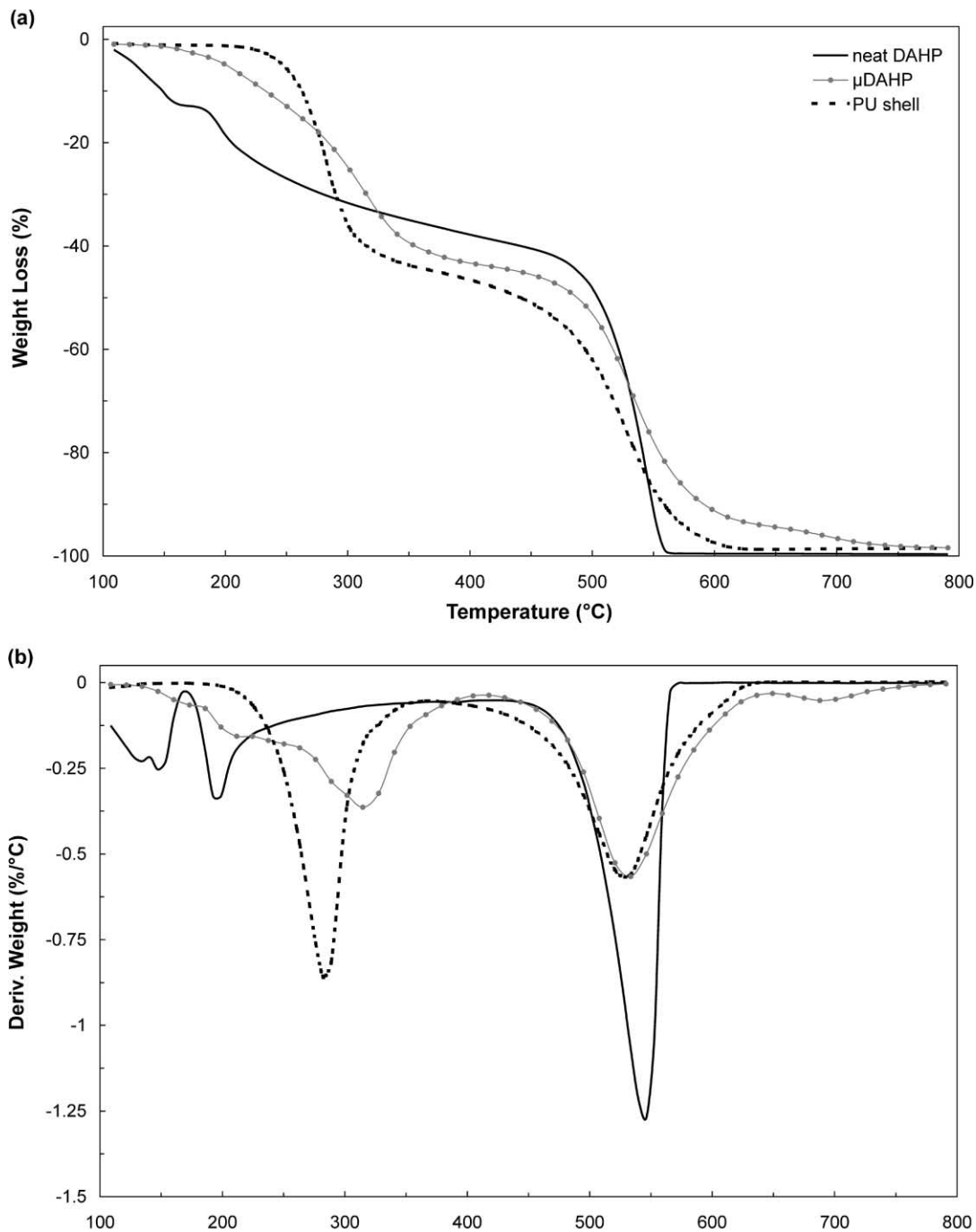


Fig. 1. TG and DTG curves of neat DAHP, microcapsules of DAHP with PU shell, and PU shell of microcapsules without DAHP.

formation of cross-linked char. From 300 °C, the thermal stability and the char residue of PU formulations are improved with the increase of neat DAHP or encapsulated DAHP loading. Thus at 450 °C, the char residue for 50/50 PU-DAHP, 60/40 PU-DAHP, 60/40 PU- $\mu$ DAHP, and 70/30 PU- $\mu$ DAHP formulations is respectively 42, 33, 30 and 28%. We can observe for 50/50 PU-DAHP and 60/40 PU- $\mu$ DAHP formulations that the peak of weight loss rate at 325 °C ( $10\% \text{ min}^{-1}$ ) is decreased by more 50% in regard to virgin commercial

PU. At 600 °C, 50/50 PU-DAHP and 60/40 PU-DAHP formulations show 15% char residue. The latter is 7% and 2.5% for 60/40 PU- $\mu$ DAHP and 70/30 PU- $\mu$ DAHP formulations respectively. Concerning the last step of degradation, we can also observe that the peak at 520 °C of weight loss rate for virgin PU is delayed at least 40 °C for 50/50 PU-DAHP, 60/40 PU-DAHP and 60/40 PU- $\mu$ DAHP formulations.

Fig. 3 shows the weight difference curves (explained in the part of TGA experiment) for the four loaded PU

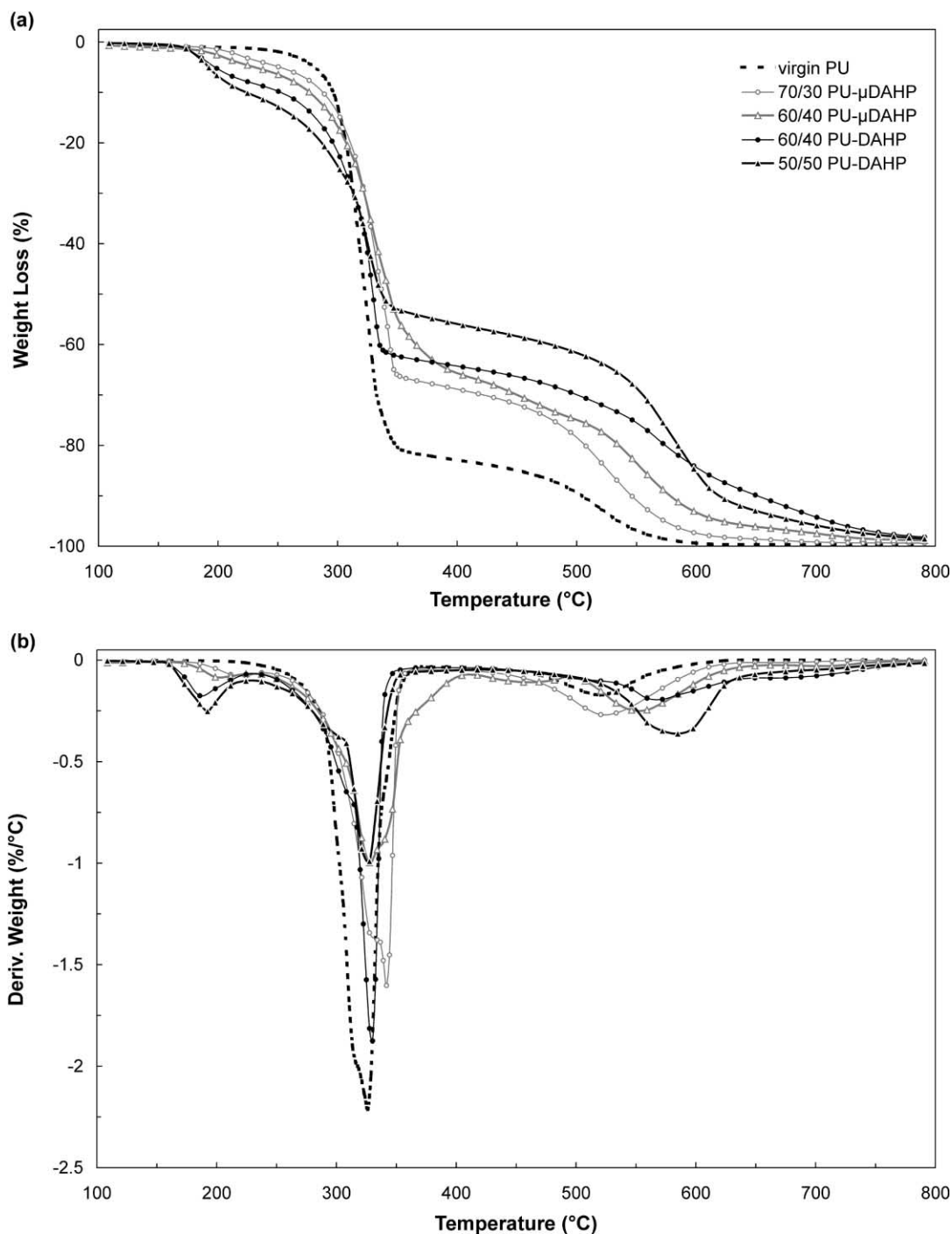


Fig. 2. TG and DTG curves of PU formulations with different loads of neat or microencapsulated DAHP.

formulations. These curves allow us to investigate interactions between the different components. The weight loss difference for PU-DAHP formulations in the temperature range 100–250 °C is positive. Indeed, there is no weight loss due to the evolving water adsorbed on the isolated DAHP. Moreover the quantity of evolving ammonia is weaker because it is retained partially by the PU coating. At 300 °C, PU-DAHP formulations have a

small destabilisation that can be attributed to development of intumescent formulation. Then PU-DAHP formulations in particular 50/50 are stabilised in the temperature range 350–800 °C with an important quantity of thermal stable char produced from reaction between the products of decomposition for PU and DAHP (maximal difference weight 27% around 550 °C). We can observe a strong stabilisation of PU- $\mu$ DAHP formulations in the

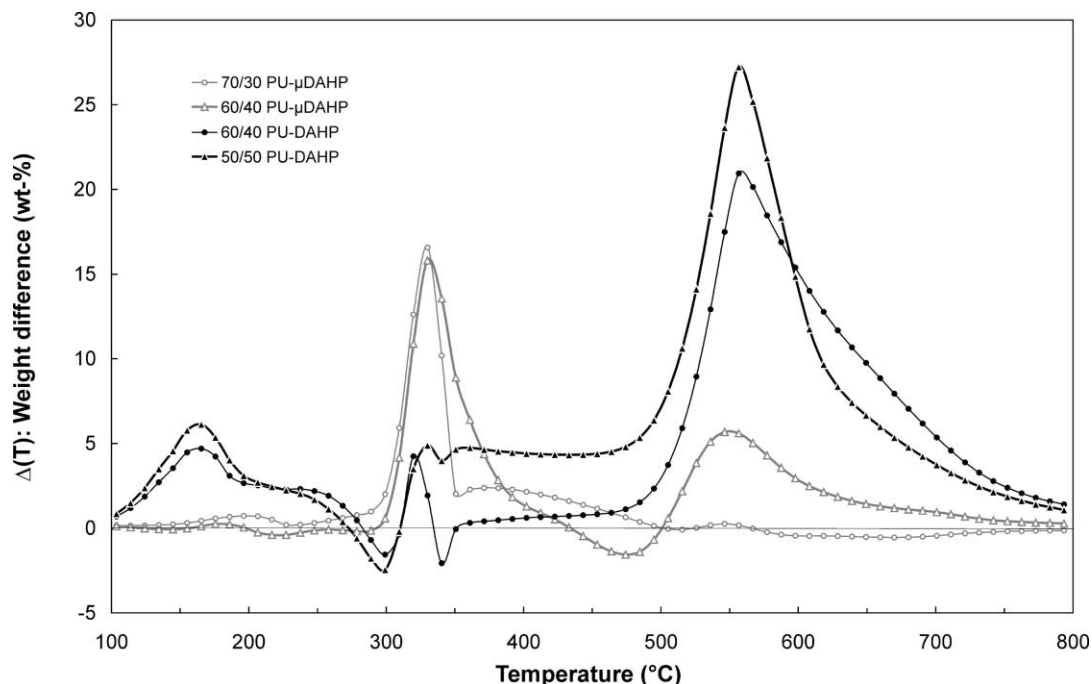


Fig. 3. Curves of weight difference for PU formulations with different loads of neat or microencapsulated DAHP.

temperature range 300–400 °C. For the same loading, the quantity of DAHP is weaker for PU loaded with microcapsules than PU loaded with neat DAHP. Thus we can suppose that the quantity of DAHP is not enough in the case of 70/30 PU- $\mu$ DAHP formulation to have an appreciable stabilisation at high temperature. 60/40 PU- $\mu$ DAHP formulation shows an interesting stabilisation in temperature range 500–800 °C with a maximum of 5% at 550 °C.

TGA experiments were also carried out on cotton coated by commercial PU and the four PU formulations, 40 or 50 wt.% of neat DAHP and 30 or 40 wt.% of encapsulated DAHP (Fig. 4). The analysis of the results obtained on cotton fabric indicates that the decomposition takes place in two stages: a very fast main stage with a maximum rate of weight loss (27%  $\text{min}^{-1}$ ) at 330 °C, representing 70% weight loss; and from 440 °C a second degradation stage accounting for 15% of the original weight of sample. The weight loss of cotton coated by virgin PU is almost a linear combination of weight loss for cotton and PU analysed separately. With respect to cotton fabric coated by neat PU, the first degradation stage of cotton fabrics coated by the four formulations of loaded PU starts earlier (180 °C instead of 250 °C). Especially for 50/50 PU-DAHP coating, the peak of weight loss rate is 18%  $\text{min}^{-1}$  at 295 °C instead of 31%  $\text{min}^{-1}$  at 315 °C for virgin PU coating. From 320 °C, the thermal stability of cotton with loaded PU coating is improved with increased neat DAHP or encapsulated DAHP loading. For 50/50 PU-DAHP, 60/40 PU-DAHP, 60/40 PU- $\mu$ DAHP, 70/30

PU- $\mu$ DAHP and virgin PU coatings, the char residue is respectively 37, 32, 24, 20 and 14% at 450 °C, and at 600 °C after the second degradation stage 21, 15, 2, 1.5 and 0%. We can consider in the case of cotton coated by PU-DAHP formulations that the end of the second degradation stage is strongly delayed up to 700 °C (3% of residue at 750 °C).

Fig. 5 is the weight difference curve for cotton fabrics coated by the different PU formulations. All the samples show an important zone of destabilisation in the temperature range 250–350 °C. But the DAHP-PU coatings are the only formulations to have a positive weight loss zone from 350 to 800 °C showing the strong interaction between cellulose and phosphate. The degradation mechanism of cotton fabrics flame retarded with inorganic phosphorus salts has been studied extensively [22–25]. Cellulose undergoes successive reactions catalysed by phosphoric acid or PPA, leading to stable conjugated unsaturated structures, which are precursors for the formation of char. Thus, as for polyurethane, cellulose forms in the presence of phosphates important quantity of char with a significant decrease of volatile flammable products. Encapsulated DAHP certainly develop char only with PU coating. With respect to PU-DAHP formulations, PU- $\mu$ DAHP formulations have for a same loading a quantity of phosphate not high enough in order to develop char also with cotton. Moreover we can suppose that DAHP is much less available for cotton in the case of formulations with encapsulated DAHP than in the case of formulations with neat DAHP.

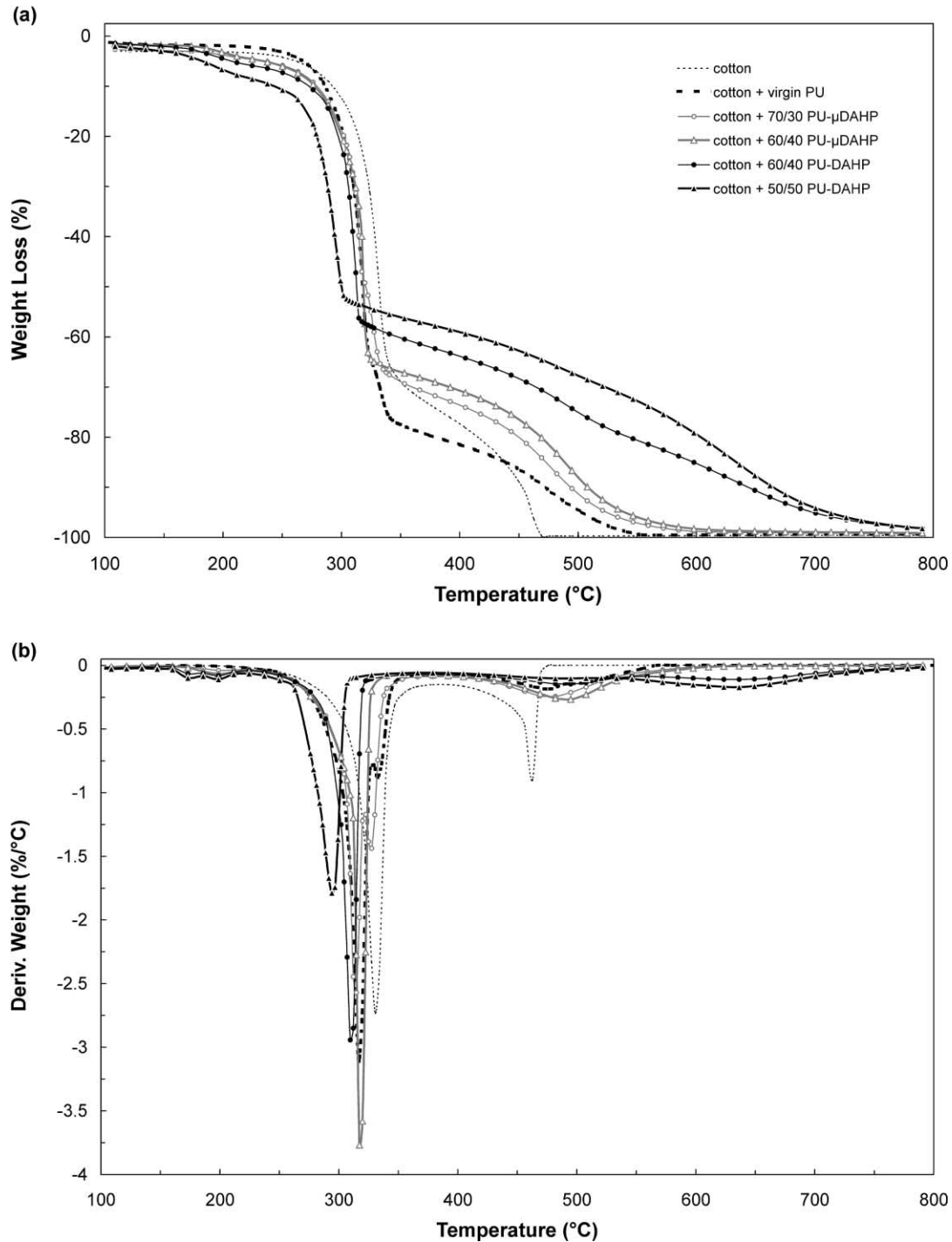


Fig 4. TG and DTG curves of cotton fabric non-coated and coated with different PU formulations loaded with neat or microencapsulated DAHP.

### 3.2. Reaction to fire of cotton fabrics coated by FR PU

The rate of heat release (RHR) is recognised to be the most important factor quantifying the size of a fire [14]. RHR curves (Fig. 6) show that a significant FR effect is obtained in the case of cotton coated by PU loaded with the DAHP microcapsules. Cotton coated by virgin PU shows a RHR peak at  $340 \text{ kW m}^{-2}$ . With respect to cotton coated by virgin PU, the RHR peak decreases by

10% with 85/15 PU- $\mu$ DAHP coating and by almost 25% with 70/30 PU- $\mu$ DAHP coating. As far as PU-DAHP coatings are concerned, the RHR peak decreases by 20% with formulation 80/20 and almost 45% with formulation 60/40. For the same loading of neat DAHP or DAHP microcapsules, the quantity of DAHP incorporated in the PU coating is smaller in the case of microcapsules. In comparison with DAHP used alone in PU coating, the performance may be assumed similar. If the

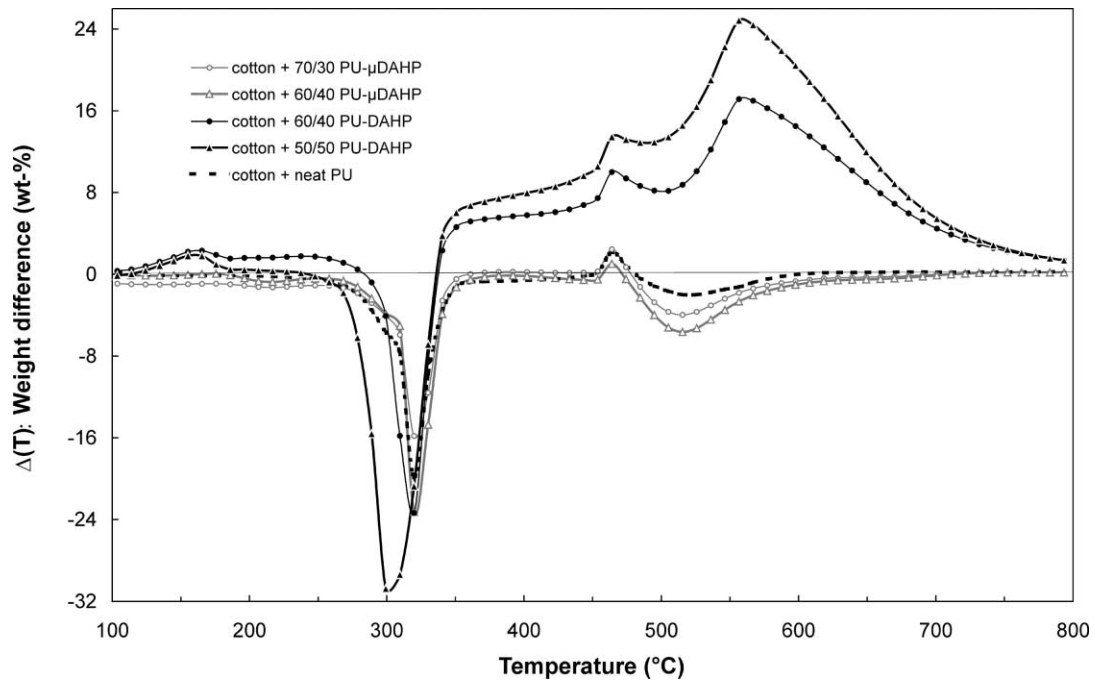


Fig. 5. Curves of weight difference for cotton fabric coated with different PU formulations loaded with neat or microencapsulated DAHP.

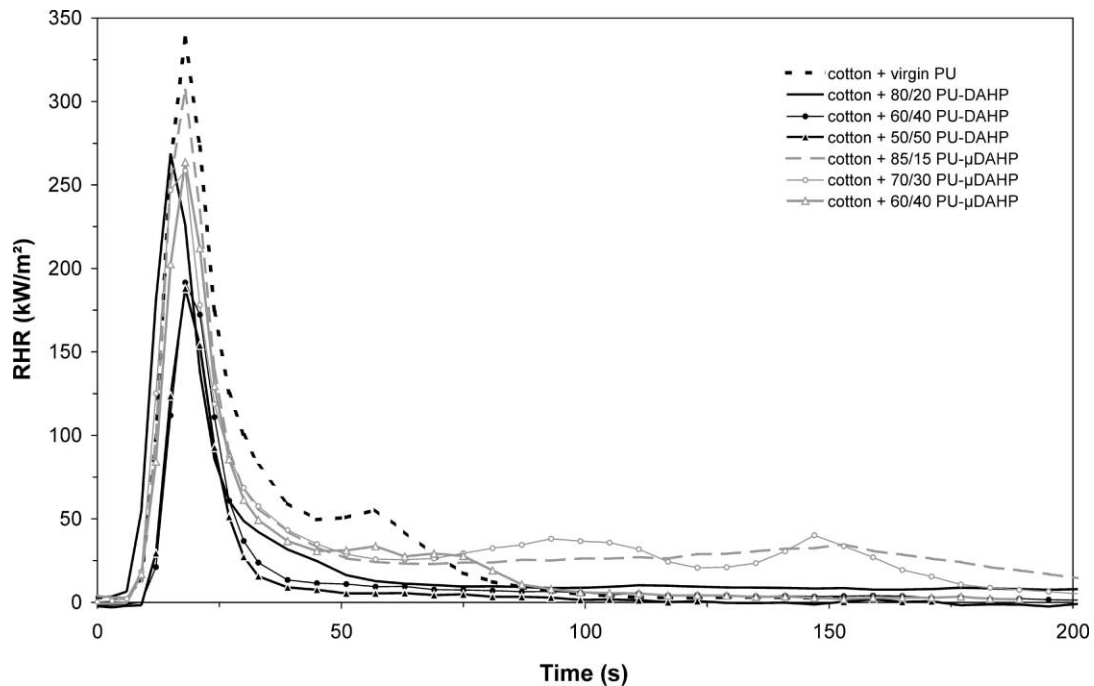


Fig. 6. RHR curves of different PU coatings on cotton fabrics.

RHR peak value is approximately considered inversely proportional to the quantity of neat DAHP loading, 15 and 30 wt.% loading of microcapsules corresponds approximately to 8 and 18 wt.% neat DAHP respectively in the PU coating. But the RHR peak does not decrease any more for 60/40 PU- $\mu$ DAHP coating in regard with 70/30 PU- $\mu$ DAHP coating. In the same way, the RHR peaks of coating with 60/40 and 50/50 PU-DAHP are equal.

It is worth noting that a second peak is observed for Virgin PU and PU- $\mu$ DAHP coatings. In the case of virgin PU coating, this second peak appears quickly followed by the total decomposition of the sample. The second peak for 85/15 PU- $\mu$ DAHP is very flat and occurs at longer time (150 s). For the 70/30 PU- $\mu$ DAHP, the second peak occurs at 90 s, then a third peak occurs 145 s. We can think that the intumescent



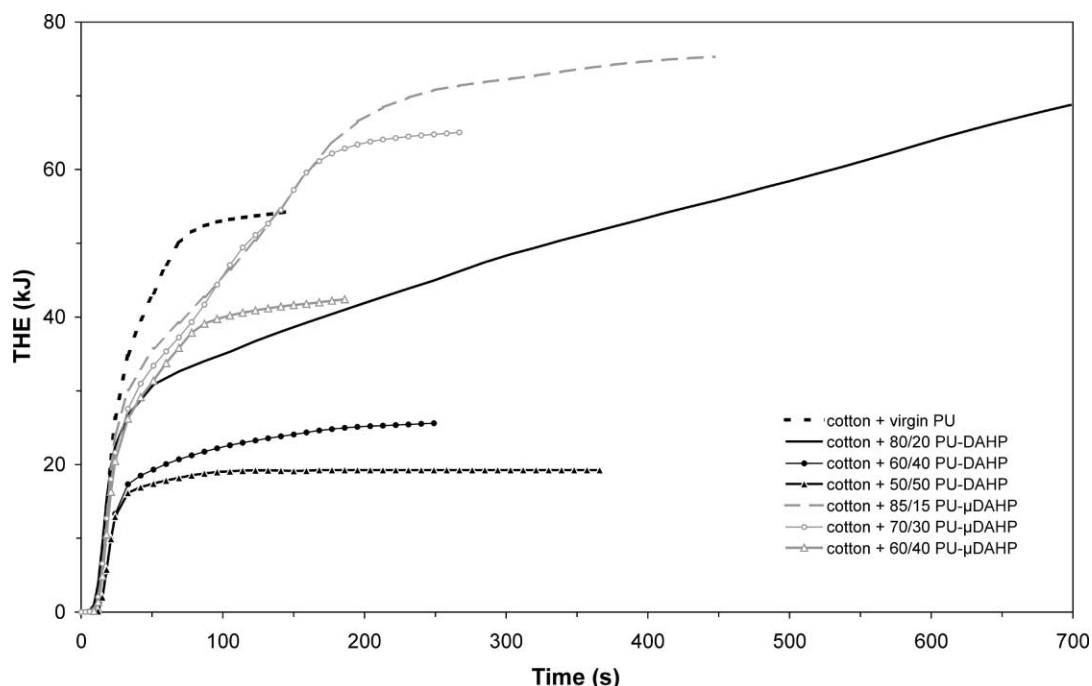


Fig. 7. THE curves of different PU coatings on cotton fabrics.

system is not strong enough because all these peaks correspond to a crack of the intumescent char with a part resumption of the combustion. It is interesting to note that in contrast to the other PU- $\mu$ DAHP coatings, the rate of heat released for 60/40 PU- $\mu$ DAHP is low as early as 90 s, after two peaks. At the same time, coatings with 40 and 50% DAHP have a low rate of heat release and their RHR curves do not present any additional peak. It means that the intumescent system is more resistant to heat and flame stresses.

Fig. 7 presents the total heat evolved (THE) for all coating formulations. As early as 25 s, THE of 50/50 PU-DAHP coating is still practically unchanged, three times weaker than THE of virgin PU coating (55 kJ). THE of 60/40 PU-DAHP coating is quite similar to 50/50 PU-DAHP coating. Those latter coatings show the best fire resistance. Until 400 s, THE of 80/20 PU-DAHP is weaker than virgin PU coating, but THE increases continuously up to 68 kJ at the end of combustion. For 85/15 and 70/30 PU- $\mu$ DAHP coatings, THE is weaker than virgin PU coating until 140 s but combustion continues and finally THE reaches 75 and 65 kJ respectively. The end of combustion for 60/40 PU- $\mu$ DAHP coating shows a lower THE (43 kJ) than virgin PU coating. This means that 60/40 PU- $\mu$ DAHP coating provides not only a flame retardant effect but also an enhancement of fire resistance.

The fire growth rate (FIGRA) index is a good indicator of the contribution to fire growth of a material. FIGRA curves of the PU coatings are shown in Fig. 8.

All coatings have a peak between 15 and 18 s. From 50 s their FIGRA is close to zero meaning that they have no contributing to the propagation of fire. Nevertheless, we can observe that the contribution to the fire growth stops faster for PU-DAHP coatings than for PU- $\mu$ DAHP coatings, and the contribution to the fire growth stops faster for PU- $\mu$ DAHP coatings than virgin PU coating. 60/40 and 50/50 PU-DAHP coatings have the same FIGRA with the smallest peak ( $84 \text{ W s}^{-1}$ ) comparatively to other coatings. It is important to note that the FIGRA peak of PU- $\mu$ DAHP coatings is inferior to the peak ( $145 \text{ W s}^{-1}$ ) of 80/20 PU-DAHP coatings which is only slightly smaller than the peak ( $152 \text{ W s}^{-1}$ ) of virgin PU coating. Moreover, among PU- $\mu$ DAHP coatings, 60/40 formulation has the smallest contribution to fire spread ( $118 \text{ W s}^{-1}$ ).

The volume of smoke production (VSP) for the coated fabrics during combustion is illustrated in Fig. 9. All the coatings evolve smoke with a main peak between 9 and 15 s. PU- $\mu$ DAHP coatings show the highest production of smoke ( $0.005\text{--}0.006 \text{ m}^3$ ). In comparison with virgin PU coating ( $0.004 \text{ m}^3$ ), smoke obscuration is lowered only with 60/40 and 50/50 PU-DAHP coatings (below  $0.0025 \text{ m}^3$ ). From 25 s these formulations have a weak but constant production of smoke, whereas PU- $\mu$ DAHP formulations do not release any more smoke.

Figs. 10 and 11 show the CO production versus time and the total quantity of CO (TCO) evolved respectively in the experimental conditions of the cone calorimeter,

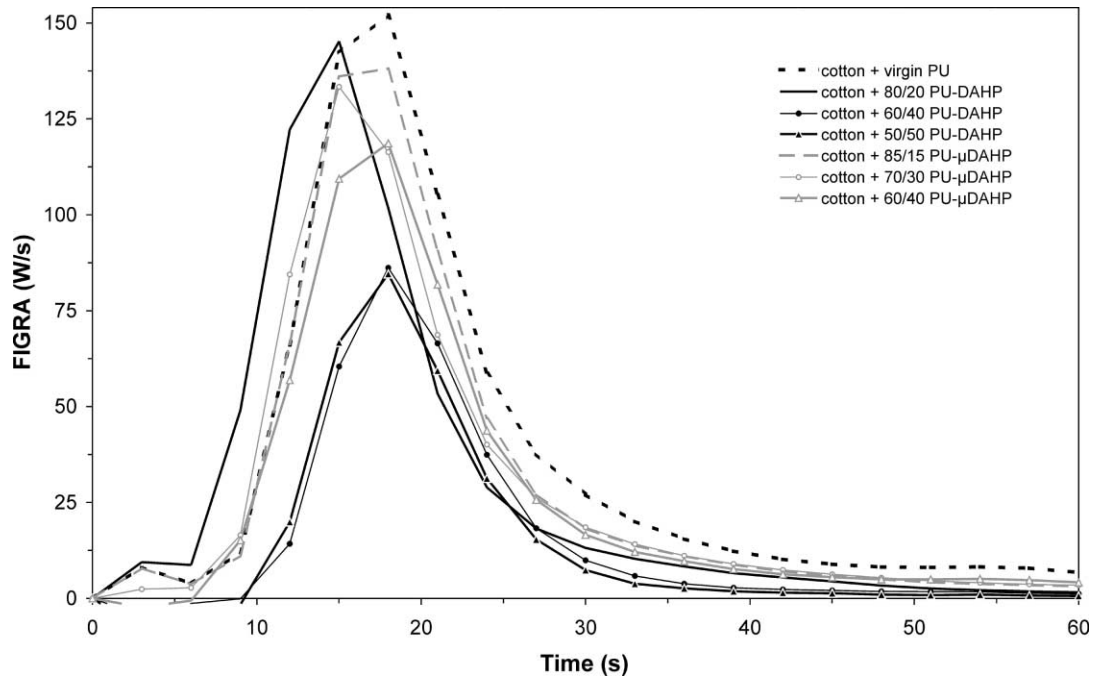


Fig. 8. FIGRA curves of different PU coatings on cotton fabrics.

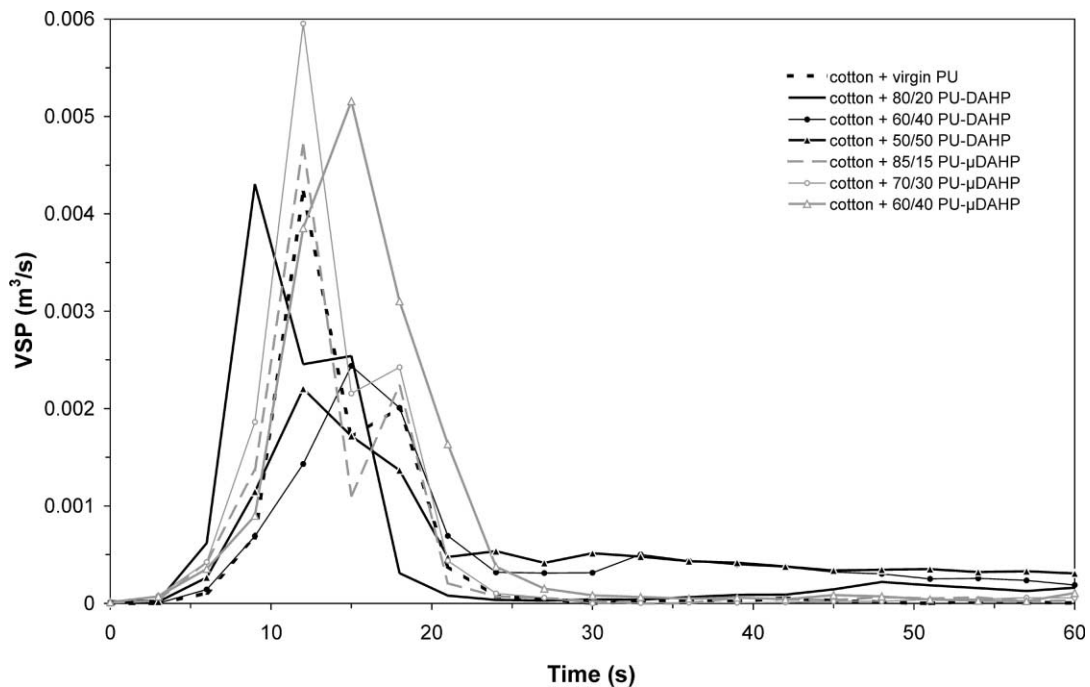


Fig. 9. VSP curves of different PU coatings on cotton fabrics.

close to the conditions of a well ventilated room. From 125 s, the total release of CO for all FR coatings is more significant than for virgin PU coating. Indeed, FR coatings release more CO due to an incomplete combustion related to the development of the intumescent system. However we observe that the higher the loading in neat or encapsulated DAHP is, the lower the total

production of CO at the end of combustion is. 80/20 PU-DAHP coating has the biggest raised production ( $34 \text{ cm}^3$ ). Then we have the following decreasing total quantity of CO for the other coatings: 85/15 PU- $\mu$ DAHP ( $30 \text{ cm}^3$ ), 70/30 PU- $\mu$ DAHP ( $26 \text{ cm}^3$ ), 60/40 PU-DAHP ( $23 \text{ cm}^3$ ), 60/40 PU- $\mu$ DAHP ( $21 \text{ cm}^3$ ), and 50/50 PU-DAHP ( $19 \text{ cm}^3$ ). It is notable that in spite of a

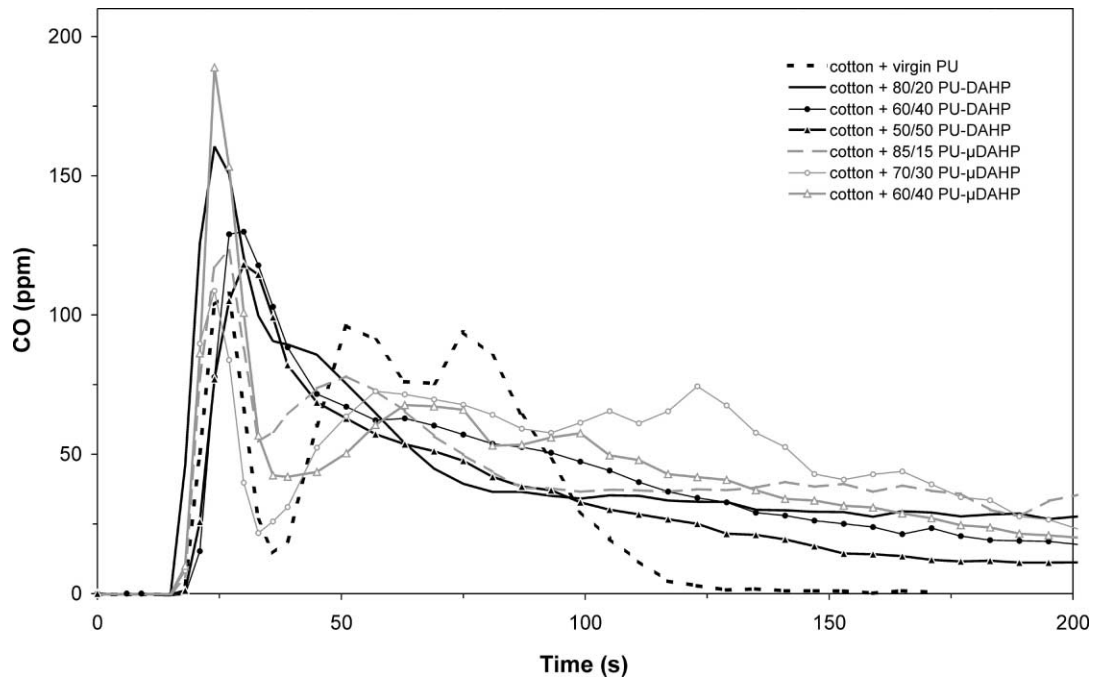


Fig. 10. CO curves of different PU coatings on cotton fabrics.

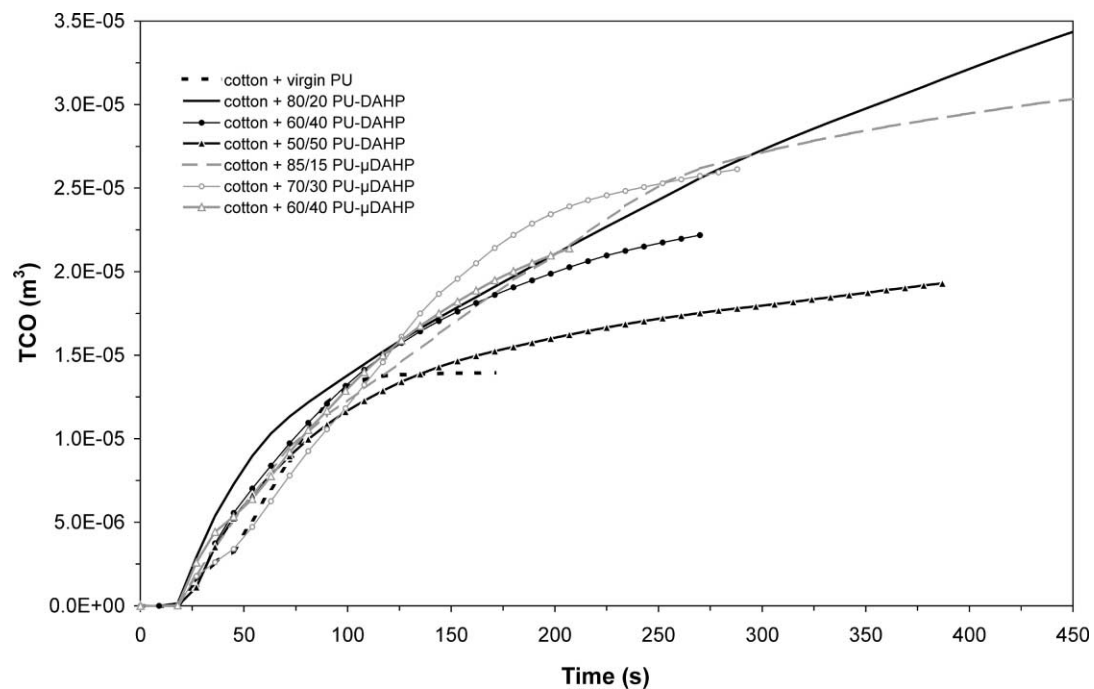


Fig. 11. Total evolved CO curves of different PU coatings on cotton fabrics.

high peak of CO release at 24 s, 60/40 PU- $\mu$ DAHP coating does not produce high quantity of CO at the end of combustion.

Figs. 12 and 13 present respectively the  $\text{CO}_2$  production versus time and the total quantity of  $\text{CO}_2$  (TCO<sub>2</sub>) evolved. At 27 s, we observe the main peak of  $\text{CO}_2$  for all the coatings. The peak of virgin PU coating is higher than that of PU-DAHP coatings and smaller than that

of PU- $\mu$ DAHP coatings. For 85/15 and 70/30 PU- $\mu$ DAHP coatings, the final quantity of produced  $\text{CO}_2$  is more than 340 cm<sup>3</sup> i.e. quite higher than one of virgin PU coating (260 cm<sup>3</sup>). We can observe that 60/40 PU- $\mu$ DAHP presents a final quantity of  $\text{CO}_2$  (185 cm<sup>3</sup>) little smaller than 80/20 PU-DAHP coating. The 60/40 and 50/50 PU-DAHP coatings product the smallest quantity of  $\text{CO}_2$  respectively 120 and 85 cm<sup>3</sup>.

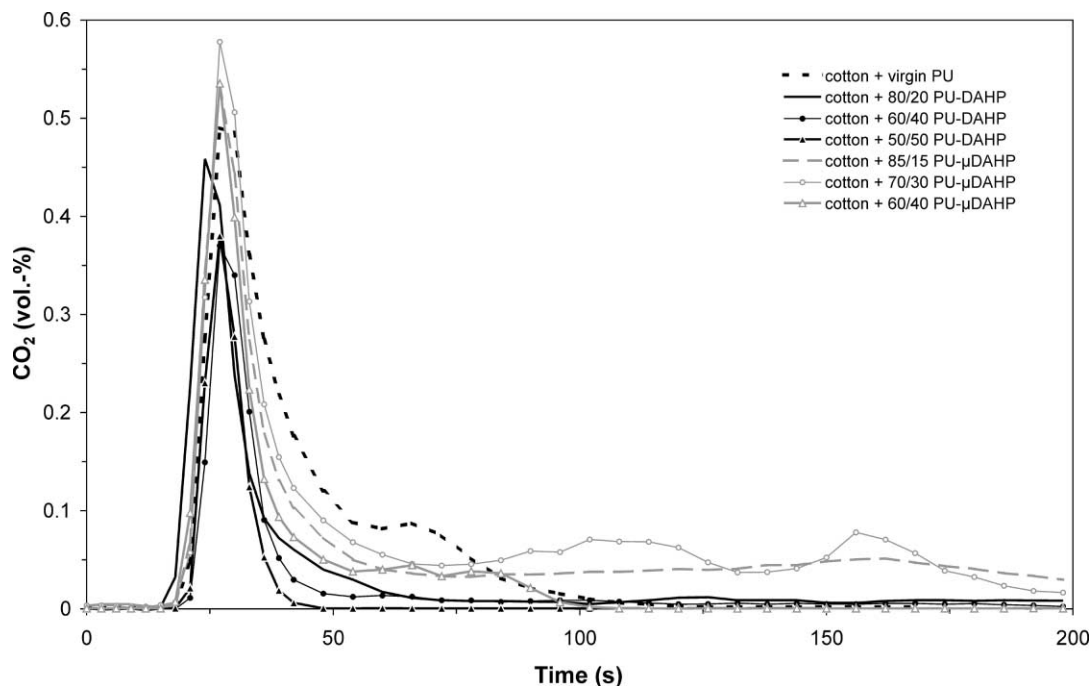


Fig. 12. CO<sub>2</sub> curves of different PU coatings on cotton fabrics.

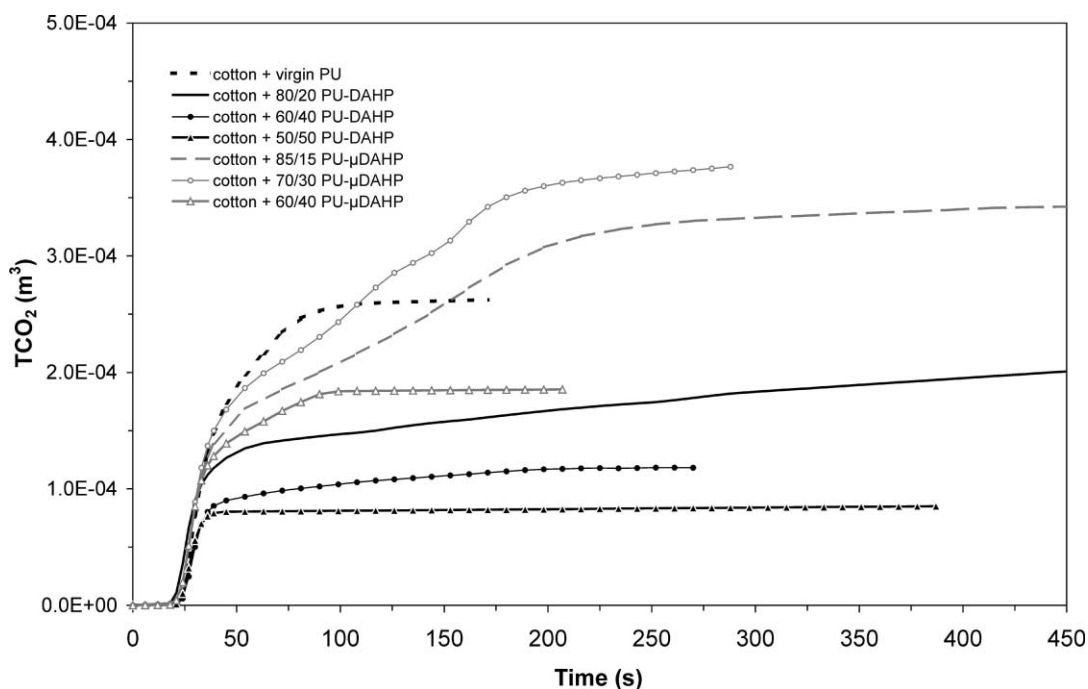


Fig. 13. Total evolved CO<sub>2</sub> curves of different PU coatings on cotton fabrics.

#### 4. General discussion and conclusion

Microcapsules of di-ammonium hydrogen phosphate with PU shell were evaluated as FR intumescent agent in a commercial PU coating for textiles. The expected advantages of this new concept of encapsulated FR agent are to be compatible with polymeric matrix to

give a permanent FR effect and to be itself an efficient FR intumescent formulation for many materials. We showed that the thermal stability of commercial PU for textile coating is improved by loading of encapsulated DAHP, in particularly with a ratio 60/40 PU- $\mu$ DAHP. In comparison with encapsulated DAHP, the thermal stability of commercial PU with neat DAHP is more sig-

nificant because the DAHP quantity is higher in formulations with neat DAHP than in formulations with encapsulated DAHP for a same loading. We studied heat and fire resistance of cotton coated by FR PU containing different ratio of neat or encapsulated DAHP. The thermal degradation of cotton fabric coated by commercial PU loaded with neat or encapsulated DAHP is delayed to higher temperature than for cotton coated by virgin commercial PU. Nevertheless in contrast to neat DAHP formulations, encapsulated DAHP formulations did not really show an increase of the thermal stability. Indeed contrary to neat DAHP formulations for the same loading, the quantity of DAHP for encapsulated DAHP formulations is not enough to develop interactions both with cotton and commercial PU. Moreover encapsulated DAHP is less available than neat DAHP to develop char with cotton. The results obtained with cone calorimeter as fire model confirm thermal analyses. The coatings with neat DAHP and encapsulated DAHP give a significant flame retardant effect with regard to virgin PU coating. But in comparison with encapsulated DAHP formulations, neat DAHP formulations present a stronger enhancement of fire resistance. We can suppose that encapsulated DAHP develop intumescent system only with PU and this FR intumescent system is not strong enough to resist to heat and flame stresses (formation of cracks in the intumescent structure). The cotton coated by the formulation 60/40 PU- $\mu$ DAHP presents several elements proving the formation of a more efficient intumescent system than other PU- $\mu$ DAHP formulations. Further work is going on to improve the formulation in particular to increase the encapsulation yield of DAHP.

### Acknowledgements

We are grateful to European project FLAMERET (“New Surface Modified Flame Retarded Polymeric Systems to Improve Safety in Transportation and Other Areas”) for its financial support.

### References

- [1] Bugajny M, Le Bras M, Bourbigot S, Poutch F, Lefebvre JM. *J. Fire Sci* 1999;17:494.
- [2] Bugajny M, Le Bras M, Bourbigot S. *J. Fire Sci* 2000;18:7.
- [3] Bugajny M, Le Bras M, Noël A, Bourbigot S. *J Fire Sci* 2000;18(1):1.
- [4] Bras Le, Bugajny M, Lefebvre M, Bourbigot JMS. *Polym Int* 2000;49:1115.
- [5] Thie C. *Encyclopedia of polymer science and engineering, microencapsulation*, 2nd ed. New York: John Wiley and Sons, 1987.
- [6] Jansen LJJM, Nijenhuis K Te. *J Membr Sci* 1992;65:59.
- [7] Jansen LJJM, Nijenhuis K Te, Boersma A. *J Membr Sci* 1993;79:11.
- [8] Giraud S, Bourbigot S, Rochery M, Vroman I, Tighzert L, Delobel R. *J Ind Text*, in press.
- [9] Arshady R. *J Microencapsulation* 1989;6:13.
- [10] Hong K, Park S. *React Funct Polym* 1999;42:193.
- [11] Frere Y, Danicher L, Gramain P. *Eur Polym J* 1998;34:193.
- [12] Babrauskas V. Development of cone calorimeter—a bench scale rate of heat release based on oxygen consumption, NBS-IR 82–2611. US Nat. Bur. Stand., Gaithersburg 1982.
- [13] Babrauskas V. *Fire and Materials* 1984;8(2):81.
- [14] Babrauskas V, Grayson SJ. *Heat release in fires*. London, UK: Elsevier Science Publishers Ltd, 1992.
- [15] CENT/TC127N 1424, Reaction to fire tests on building products (“SBI” test), Draft 26 February 1999.
- [16] Kishore K, Mohandas. *Combustion and Flame* 1981;43:145.
- [17] Grassie N, Perdomo Mendoza GA. *Polym Degrad Stab* 1985;10:267.
- [18] Grassie N, Zulfiqar M. In: Scott G, editor. *Developments in polymer stabilization*, Vol. 1. London, UK: Applied Science Publishers, 1979.
- [19] Grassie N, Perdomo Mendoza GA. *Polym Degrad Stab* 1985;10:43.
- [20] Grassie N, Perdomo Mendoza GA. *Polym Degrad Stab* 1985;11:145.
- [21] Grassie N, Perdomo Mendoza GA. *Polym Degrad Stab* 1985;11:359.
- [22] Grassie N, Scott G. *Polymer degradation and stabilisation*. Cambridge, UK: Press Syndicate of the University of Cambridge, 1985.
- [23] Farooq AA, Price D, Milnes GJ, Horrocks AR. *Polym Degrad Stab* 1991;33:70.
- [24] Farooq AA, Price D, Milnes GJ, Horrocks AR. *Polym Degrad Stab* 1994;44:323.
- [25] Khatib MA, Kandil SH, Gad AM, El-Latif M, Morsi SE. *Fire and Materials* 1992;16:23.